

## **A Cell Level Model for Battery Simulation**

Suguna Thanagasundram<sup>1</sup>, Raghavendra Arunachala<sup>1</sup>, Kamyar Makinejad<sup>1</sup>, Tanja Teutsch<sup>2</sup>,  
Andreas Jossen<sup>2</sup>

<sup>1</sup>*TUM CREATE Centre of Electromobility, 1 CREATE Way, #10-02, CREATE Tower, Singapore 138602  
suguna.thanagasundram@tum-create.edu.sg*

<sup>2</sup>*Institute for Electrical Energy Storage Technology, Technische Universität München, Arcisstrasse 21, 80333 Munich,  
Germany*

---

### **Abstract**

An equivalent circuit model is the most common and straight-forward way of representing the dynamic behaviour of a lithium-ion battery. In literature, many examples of circuits are proposed and various techniques are also discussed for parameterisation of the models. In this paper a second order equivalent circuit is proposed and the parameters identification method by Hybrid Power Pulse Characterization (HPPC) testing is described. The modelling and parameter identification process is done in the Matlab/Simscape environment. This non-linear model encapsulates the dynamic electrical behaviour of a typical automotive cell. A validation process is carried out to benchmark the voltage errors between estimated voltage profile of the battery cell model and actual cell measurements. The comparison between measurement and simulation shows a good accordance. The current pulse technique is also presented to verify the ohmic resistance values obtained by the optimisation process in the parameters identification method. A study is also conducted to investigate how cell chemistry affects the proposed model.

*Keywords: Battery Electric Vehicle (BEV), lithium battery, modelling, battery model, internal resistance*

---

### **1 Introduction**

The ever increasing demand for limited fossil fuels and growing concerns over the CO<sub>2</sub> emission have spurred worldwide interests in developing alternative energy and storage systems, particularly for Electric Vehicles (EV) and Hybrid Electric Vehicles (HEV) application. Lithium-ion battery is a promising power source for EVs and HEVs due to its high energy density, long cycle life and low self-discharge. The integration of lithium-ion batteries in EV and HEV applications require a dynamic model which predicts the performance of the battery at different operating conditions in order to

optimize the energy usage and prolong its useful life.

Researchers around the world have developed a wide variety of techniques with varying degrees of complexity to model the battery. Battery models can be classified into electrochemical models (chemistry-based), mathematical models and electrical models (circuit-based). Chemistry-based models are derived from porous electrode theory and concentrated solution theory proposed by Newman and Tiedemann [1] and Doyle et al. [2] which mathematically describe the charge/discharge processes and transport kinetics in the solid and electrolyte phases in the battery as simplified 1D spatial structures. These models have the ability to accurately predict the performance of battery. However they require a

detailed understanding of complex electrochemical processes, often involving a large number of algebraic equations and state variables to model the battery behaviour. Chemistry-based models are commonly developed using Finite Element Analysis Software such as Ansys and Comsol [3, 4]. In cell design studies, chemistry-based models are used to determine optimal parameters of the cell such as the form factor or electrode thickness. They can also be used at the pack level to aid in the design of the battery system or to determine rate of coolant flow inside the modules to maintain the cells at a safe operating temperature within the limits of a certain thermal band as required by the vehicle application. The advantage of chemistry-based models is that they can be used to predict the behaviour of the cells beyond the range of experimental data e.g. thermal runaway conditions. The main drawbacks of chemistry-based models are that they are computationally time-consuming and very complex hence not applicable in EV application due to the real-time demands of Battery Management Systems (BMS).

Mathematical-based models are developed primarily using the Shepherd relation and modifications to the Shepherd model [5, 6]. These modifications usually consist of adding and altering terms of the original model to relax assumptions behind the Shepherd model. In mathematical oriented models, the parameters are extracted by curve fitting the manufacturer's discharge curves. A classic example of the mathematical model of a battery is the battery blockset in SimPowerSystems Toolbox in Matlab [7]. Mathematical-based models are simple but application dependent and not accurate enough to reproduce fast varying battery voltage dynamics.

However, circuit-based models are very useful and simple, because the complex electrochemical processes can be transformed into electrical circuit elements which describe the battery kinetics [8, 9]. Circuit-based models use electrical components such as voltage sources, resistors, capacitors and inductors to encapsulate the battery behaviour. Circuit-based models can be further classed into two main categories: Thevenin-based models and impedance-based models [10]. The Thevenin-based models are constructed by curve-fitting a set of experimental voltage and current measurements over a range of battery operating conditions whereas the

impedance-based models are developed by fitting with impedance spectra. Circuit-based models are recommended for thermal studies within the range of fitting. Circuit-based models are real-time implementable [10] and can be run on Hardware-in-Loop (HIL) platforms. Hence they are useful for BMS development and serve as a part of vehicle level simulation studies for battery pack sizing and range estimation calculations. The accuracy of circuit-based models lies between the chemistry-based and mathematical-based models.

## 2 Second Order Equivalent Circuit Model

One example of circuit based battery model is the Second Order Equivalent Circuit (SOEC) model. The schematic of the model is shown in Fig.1. There are 6 components in the model: VOC,  $R_i$  and the two parallel polarization RC network combinations, namely,  $R_1$ ,  $R_2$ ,  $C_1$  and  $C_2$ . Each component is representing a different aspect of the battery.

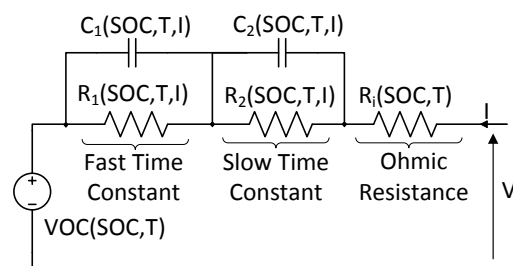


Figure 1: Second Order Equivalent Circuit (SOEC) model of a battery cell.

VOC is the Open Circuit Voltage and one of the most important parameter of a battery.  $R_i$  is the ohmic or DC resistance.  $R_i$  is representative of the internal resistance in the cell, similar to terminal resistance and electrode resistance and is responsible for the immediate voltage drop or rise when the battery is being discharged or charged.

$R_1$ ,  $C_1$ ,  $R_2$  and  $C_2$  are the two RC parallel polarization elements, responsible for the transient response of the battery [11, 12].  $R_1$  and  $C_1$  describe the fast dynamics in the battery depicting surface effects on the electrodes and reaction kinetics.  $R_1$  is the charge transfer resistance and  $C_1$  represents the electrochemical double layer capacitance.  $R_2$  and  $C_2$  represent the slower dynamics of the cells in order of hours. They are more representative of the diffusion processes in the electrolyte and active material. All these parameters are functions of the State-of-Charge (SOC) of the battery, temperature (T) and current (I).

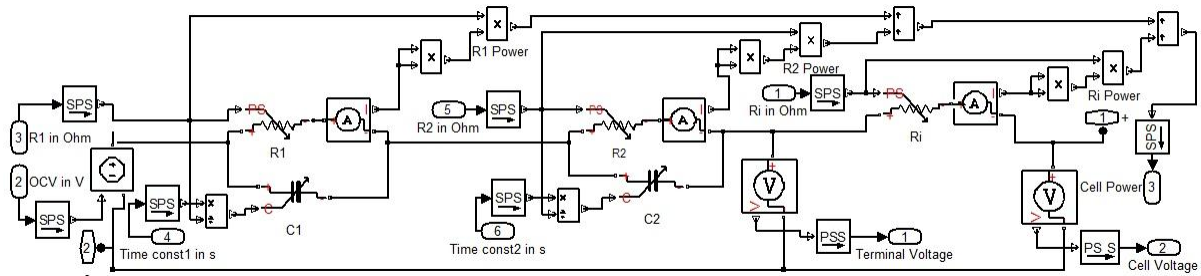


Figure 2: Implementation of the SOEC model in Simscape.

## 2.1 Non-linear dynamic SOEC Model

The SOEC model of the cell is implanted in Matlab/Simscape [13] as shown in Fig.2. Simscape, which is one of the toolboxes in the Mathworks suite of products, is a flexible, acausal and an object-oriented tool for modelling and simulating complex integrated multi-physics, multi-engineering systems. The Simscape platform was chosen because it is a physical modelling tool with multi-domain capability. This was a useful feature as one of the intended objectives of the work is to couple the electrical and thermal properties of the cell behaviour. The SOEC model in Simscape is intuitive and easy to understand as it looks just like a circuit in real-life and the solution to the model is found by symbolic reduction techniques. Additional components like resistors or capacitors can easily be added to the circuit. The preceding sections describe how the values of VOC,  $R_i$ ,  $R_1$ ,  $R_2$ ,  $C_1$  and  $C_2$  were determined for the battery SOEC model. Fig.2 shows purely the electrical model of the SOEC cell. The thermal behaviour of the cell has also been modelled in a similar way using the thermal library in Simscape but it is not shown in this paper.

## 3 Experiment Description

### 3.1 Current Pulse Techniques

The parameterization method used in the study is similar to the one described in [14, 15]. It is the current pulse technique, commonly known as the HPPC test and is described in detail in the FreedomCAR Battery Test Manual [16, 17]. This method is used to calculate the dynamic properties of a battery. The battery is charged and discharged under a controlled condition and the terminal voltage, current and temperature measurements are monitored. A HPPC test profile is shown in Fig.3.

### 3.2 Battery Cells used for the study

Tab.1 shows the specification of Lithium-ion cells of three different chemistries considered for the study. They are Lithium Cobalt Oxide (LCO), Lithium Manganese Oxide (LMO) and Lithium Iron Phosphate (LFP). LCO and LMO have higher theoretical capacity [18], compared to LFP due to the higher operating voltage. LFP cells are characterized by high intrinsic safety and that makes them suitable for high power applications.

### 3.3 Platform of Implementation

The tests were carried out on BaSyTec CTS battery tester at TUM CREATE Centre for Electromobility in Singapore. The battery tester provides an automatic and dynamic current range selection allowing non-interrupted current flow in the constant voltage mode when current decreases with charging time.

Ideally the power pulse characterisation should be done at 3C charge/discharge rate but since the battery cyclers that were available for testing were limited to 5A, the maximum charging and discharging was done at 5A. The cell rests for 3 minutes and then discharged for 6 minutes at 1 C rate (which is 2.3A in this case) to achieve a 10% decrease in SOC. Afterwards the cell rests for 1 hour to reach equilibrium before the next HPPC test profile begins. The partial discharge-HPPC-rest phase cycle is repeated at decrements of 10% of SOC till the cell reaches 10% SOC. The process is repeated in the charging direction as well. Fig.4 shows typical current, voltage and Ah plots of cell type 1 obtained from the HPPC test profile. The nominal voltage and capacity of the cell are 3.3V and nominal capacity of 2.3 Ah as stated in Tab.1. The conventions used for charging current are positive and discharging current is negative as shown in Fig.4.

## HPPC Profile

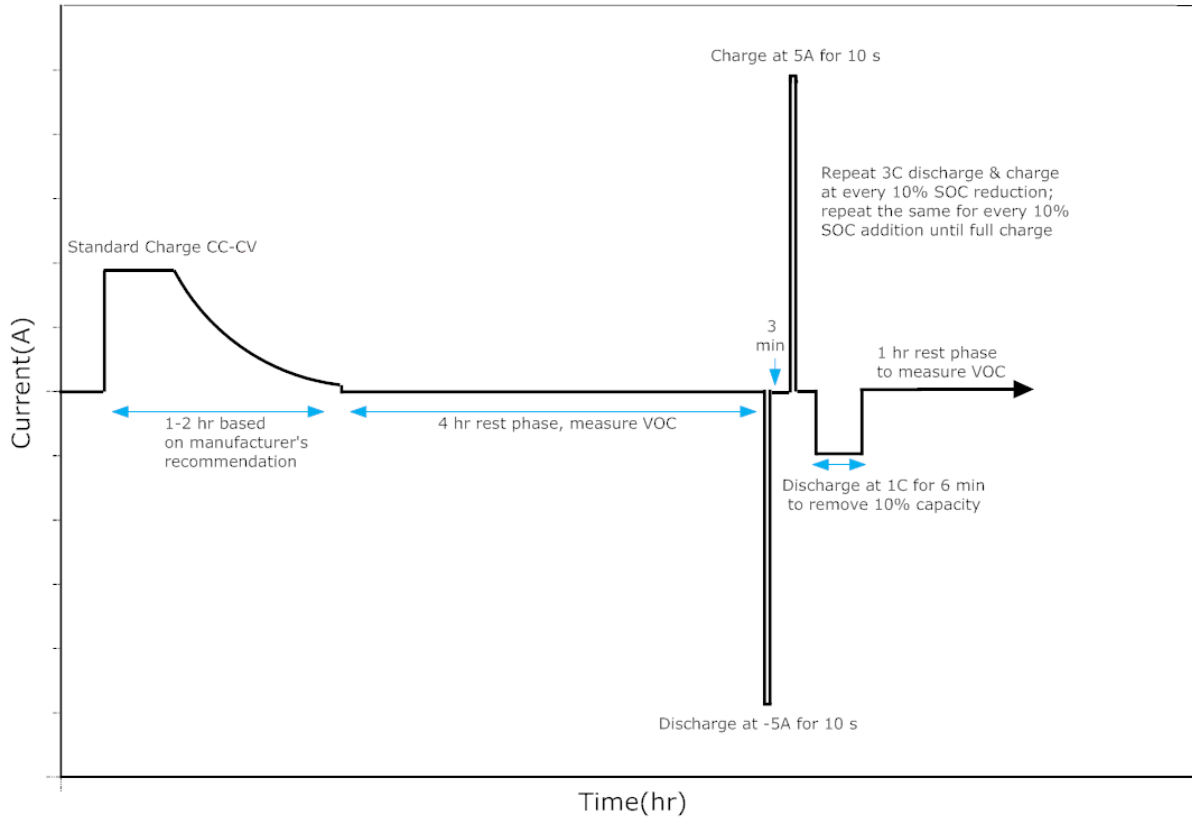


Figure 3: Hybrid Pulse Power Characterization (HPPC) test profile.

Table 1: Specification of Lithium-ion cells.

	Cell Geometry	Size (mm)	Cell Chemistry	Weight (g)	Nominal Voltage (V)	Nominal Capacity (m Ah)
Cell Type 1	Cylindrical	26 (D) 65 (H)	Lithium Iron Phosphate	70	3.3	2300
Cell Type 2	Cylindrical	18 (D) 65(H)	Lithium Cobalt Oxide	45	3.6	2250
Cell Type 3	Cylindrical	18(D) 65(H)	Lithium Manganese Oxide	44	3.6	2200

The Ah curve was recorded for balance counting. [Tab.2](#) summarizes the specifications of the BaSyTec CTS battery tester. Four wire measurement method is used to connect the test cells to the battery tester. All experiments on the cells are conducted at room temperature. The cells are preconditioned by conducting two complete cycles of charge-discharge followed by a 4 hour rest period to attain temperature and

voltage equilibrium. The measurement starts with a complete charged cell. The HPPC test profile consists of 10s pulse discharge at -5A, followed by 10s charge pulse. After each pulse discharge/charge, there is a pause for 3 minutes. Then the cell is discharged at 1 C-Rate to remove 10% of its capacity. The cell is rested for 1 hour before the next HPPC test profile begins.

Table 2 Specifications of the BaSyTec CTS battery tester.

Channels per unit	32
Four wire measurement	Yes
Maximum Charging Current (A)	5
Maximum Discharging Current (A)	-5
Voltage range during charging/discharging (V)	+5/0
Time resolution (ms)	20
Current Range (charge/discharge)	5 A/300 mA/15 mA/1 mA (Automatic and dynamic range switching)

### 3.4 SOEC Parameters Determination

The VOC is defined as the potential difference between the positive and negative electrodes of

the battery cell when there is no current flow and the cell is in an equilibrium state. The VOC is determined at different SOCs, normally at the end of each rest/relaxation phase (in this case, 1 hour) when the voltage is at steady-state and the temperature of the cell has stabilised.

The voltage of a cell under current flow is different from the VOC. The cell shows an increased voltage during charge and a decreased voltage during discharge. The difference occurs due to the polarization voltage which can be attributed to two mechanisms. One mechanism is the overpotential at the electrodes caused by electro chemical reactions and concentration deviations due to the transport phenomena in the cell. The other mechanism is an ohmic voltage drop across the current collectors and electrolyte when there is a current flow. VOC was measured on the candidate cell type 1 by giving a relaxation of 1 hour after each charge/discharge for SOC increment/decrement (Fig.5).

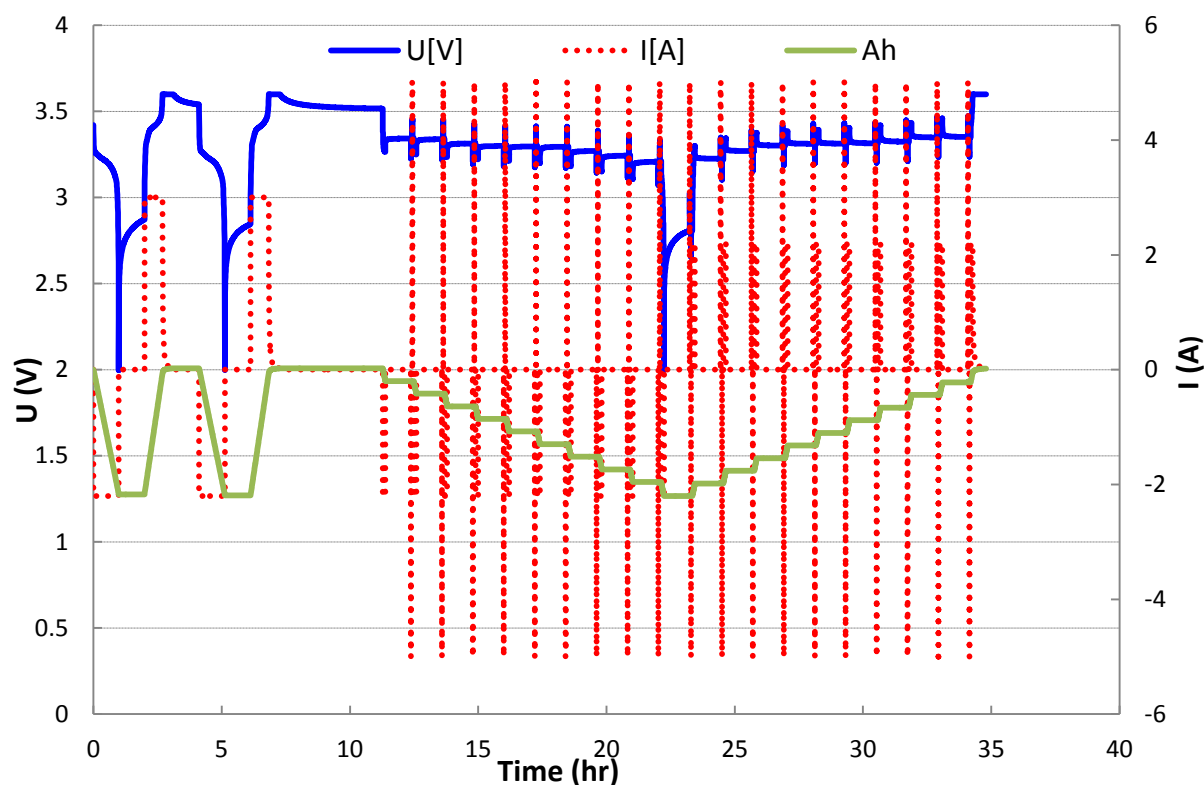


Figure 4: HPPC test profiling for Cell Type 1. Cell is discharged and charged in steps of 10% SOC. Charge and Discharge pulses are applied at each step of SOC.

Depending on whether the cell has recently undergone a charge or discharge event, the VOC is slightly different for this cell at each SOC indicating that there is some hysteresis and that the cell has not reached true steady state. Although the time period of one hour was not sufficient to truly reach equilibrium state, the 1 hour rest period was chosen as a trade-off between testing time and measurement accuracy. The true VOC is assumed to be in the area between the charged and discharged regions and for the purpose of the SOEC model, the average value of VOC is chosen by taking the mean value of charge and discharge VOC.

Other parameters of the SOEC model are evaluated by analysing the voltage response of HPPC pulse discharge and charge. Fig.6 shows the voltage response of the cell when -5A pulse is applied for a duration of 10s.

To automate the parameterization process, once a profile such as shown in Fig.4 has been obtained, a Matlab script is used to separate the measurements of HPPC test done at different SOC during charging and discharging. The 10 second pulse is further split into the short time constant  $t_1$ , representing the fast dynamics, and the long time constant  $t_2$ , representing the slow dynamics. From each of these measurements, the values of  $R_i$ ,  $C_1$ ,  $R_2$  and  $C_2$  are calculated by applying Eq.(1)-(5) to obtain initial estimates of the parameters from the zoomed curves at each steps of the SOC. These values are then fed into Eq.(6) to simulate the voltage of the battery cell.

$$R_i = (u_0 - u_1)/i \quad (1)$$

$$R_1 = (u_1 - u_2)/i \quad (2)$$

$$R_2 = (u_2 - u_3)/i \quad (3)$$

$$t_1 = R_1 C_1 \quad (4)$$

$$t_2 = R_2 C_2 \quad (5)$$

$$V_s(t) = VOC + I(t)R_i + I(t)R_1(1 - e^{-\frac{t}{t_1}}) + \quad (6)$$

$$I(t)R_2(1 - e^{-\frac{t}{t_2}})$$

$$LSE = (V(t) - V_s(t))^2 \quad (7)$$

Let  $V_s(t)$  be the simulated battery terminal voltage obtained from Eq.(6) and  $V(t)$  be the battery terminal voltage obtained from the measurement as shown in Fig.6.

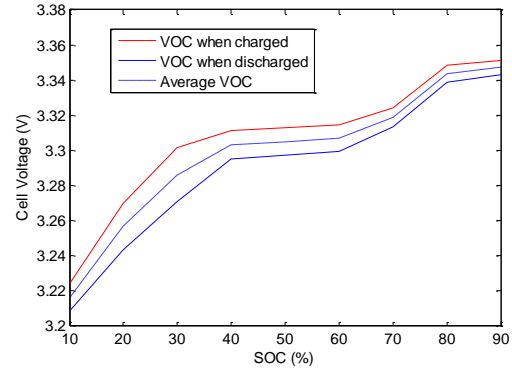


Figure 5: Measured VOC vs. SOC during charging and discharging for Cell Type 1.

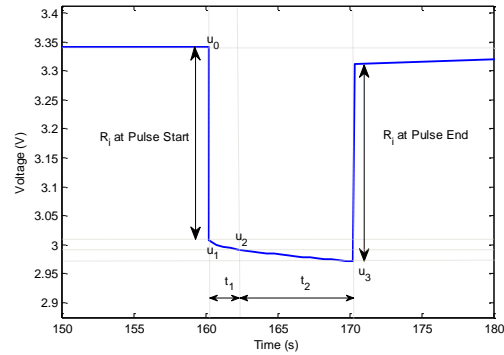


Figure 6: Voltage response to a 10s -5A discharge pulse in the HPPC test for Cell Type 1.

The difference between the measured voltage and simulated voltage is the modelling error and is defined using Eq.(7). The unconstrained optimisation algorithm fminsearch (Nelder-Mead) provided by Matlab is used to minimise the error for each of the analysed pulses and the optimized parameters  $R_i$ ,  $R_1$ ,  $C_1$ ,  $R_2$  and  $C_2$  at each state of SOC are obtained. These values are fed in the original SOEC model in Simscape to mimic the cell behaviour. The time constant of the RC parallel circuits in Fig.1 are given by  $t_1$  and  $t_2$ . They differ by an order of magnitude and therefore they are representative of the fast and slow transient dynamics of the battery cell.

### 3.5 Validation of SOEC model

#### 3.5.1 Validation of internal ohmic resistance $R_i$

Besides the automatic calculation of the internal ohmic resistance based on the developed SOEC cell model and the HPPC test results with the use of the Matlab script in this paper, other methods

and techniques are also investigated to calculate the internal resistance of the cell. The most common method of measuring the internal resistance of the cell is to use the conventional current step pulse technique. When using this method, some important consideration should be taken into account. In this method the determination of the internal resistance is based on the analysis of the immediate jump in the terminal cell voltage due to the current pulses. Input current can be in the form of short duration charging or discharging pulses. It is also possible to investigate the change in the cell terminal voltage during switching off the input current to measure the internal resistance. This method is commonly used for homogeneity tests of the lithium-ion cells in in EV and HEV applications.

With the BaSyTec battery tester system we have the possibility of measuring the internal resistance of the cell directly during the test as it is mounted on a 4 wire measuring kelvin probe cell holder. For the proper recording of these voltage jumps, a sampling rate of 1ms to 5ms [19] is necessary to increase the voltage resolution to capture minute changes in the voltage. The internal resistance can then be calculated from Eq.(1). This method was used and the results for 3 cell samples of cell type 1 (Cell 1, Cell 2 and Cell 3) LFP cells are presented in Fig.7.

For cell type 1, the maximum discharge pulse can be as high as 120A for a short duration pulse test but because of the limitation of our battery testers, we used +5/-5A to apply charge/discharge pulses to the cell. In Fig.7,  $R_i$  results are based on the discharge and charge current pulses during discharging section of the HPPC test as well as the discharge and charge pulses during the charging section of the HPPC test.  $R_i$  was calculated for both the switching on and switch off of the charge/discharge pulses. It can be seen from the results of Fig.7 that there is a general increase in  $R_i$  values as SOC reduces for all three samples of the cell type 1.

These tests can be conducted at different temperatures, but in this paper we only present the results at 20°C. To give an overview about the approximate values of the internal resistance at different temperatures, the internal resistance of a similar tested cell can be as high as 30mΩ at -20°C to 10mΩ at 35°C [20]. It is understood that the internal resistance of the battery increases

with decreasing temperature. In short, with lithium-ion batteries, the internal resistance shows a significant temperature dependency.

The  $R_i$  values in Fig.7 are also compared with the  $R_i$  values obtained from the optimization scripts mentioned in section 3.4. Refer to Fig.8 and Fig.9. Both set of values obtained from the different techniques show similar trend with higher resistances at very small SOCs, plateau in the region of 20-80% SOC and slight increase in resistance at the end at 90-100% SOC. This indicates that the optimisation script does work well and does give comparable results. The only difference was that the optimisation script gives slightly bigger resistances (about 3 mΩ higher) but this is a reasonable and acceptable limitation of the method considering the bigger changes in the resistance values that can occur if there are measurement inaccuracies or unintended contact resistance at the cell current collector terminals.

In [21], other methods of calculating the internal resistance of the cell are suggested. Electrochemical Impedance Spectroscopy (EIS), energy loss method and Joule's law technique with the aid of the Accelerated Rate Calorimeter (ARC) production of Thermal Hazard Technology (THT) company are used and compared with the results from the current pulse technique. The comprehensive tests and experiments are under investigation and out of the scope of this paper.

### 3.5.2 Comparison of the simulated and measured voltages

To validate the SOEC model, the parameters extracted from the optimisation script are used to simulate the cell voltage response for cell type 1 fed with another HPPC test profile similar to the one used for the training data. Fig.10 shows the simulated voltage response and the measured voltage measurement. Fig.11 shows the modelling error. It can be seen that SOEC model can capture the dynamic voltage response of the cell very well with a modelling error of approximately less than 3% from 10% SOC to 90% SOC. However the model response is poor at SOCs below 10% producing a big modelling error.

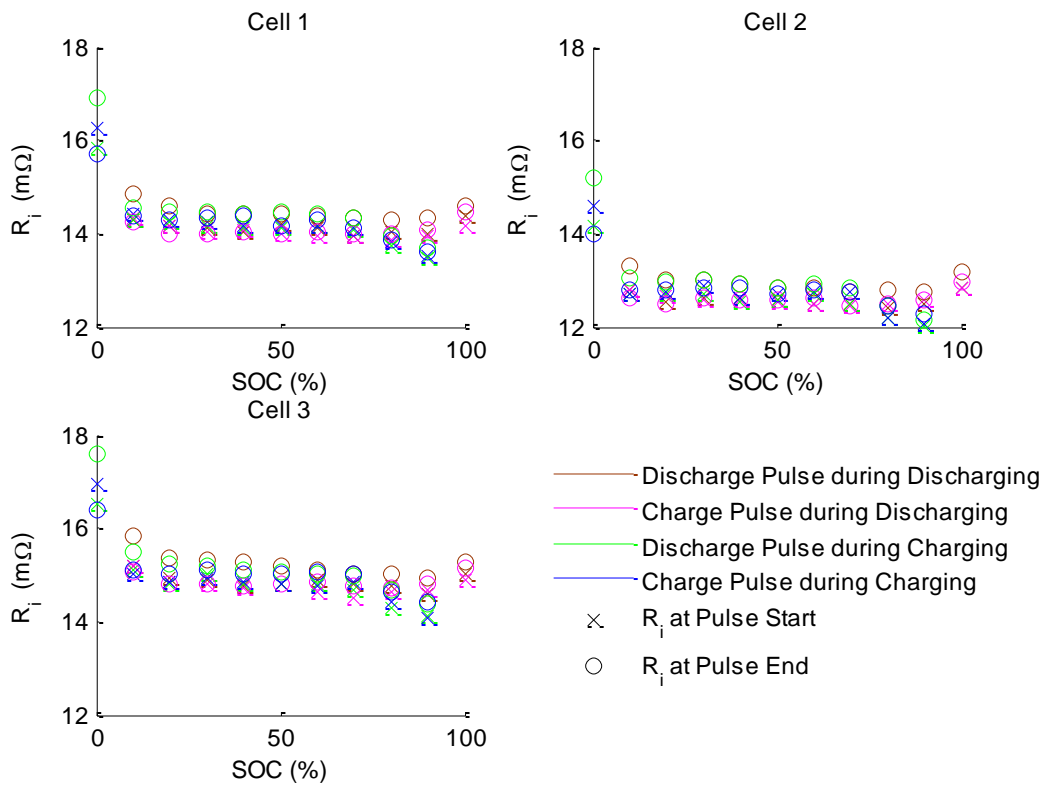


Figure 7: Internal resistance  $R_i$  measurement for Cell Type 1 based on the current charge/discharge pulses at both current switch on and switch off.

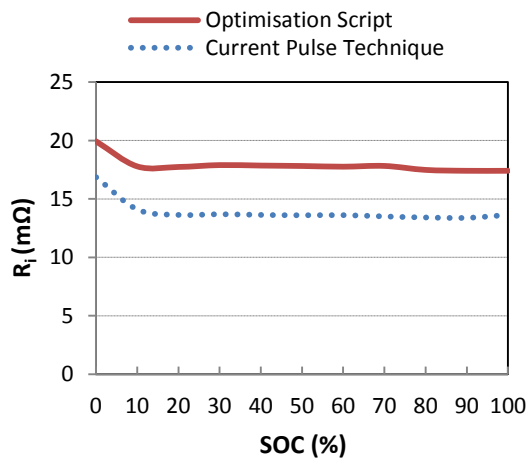


Figure 8: Measured internal resistance  $R_i$  values versus  $R_i$  values obtained from the optimization script at 10% step SOC for charge pulses.

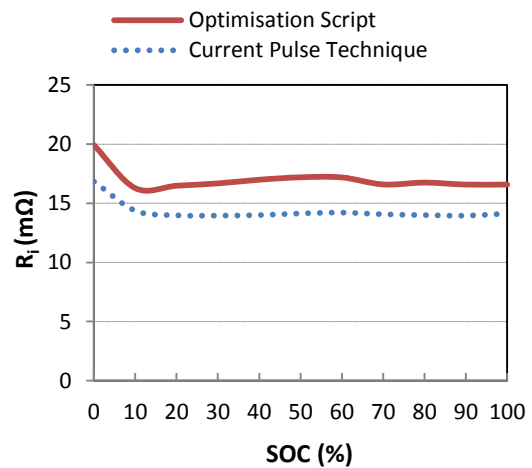


Figure 9: Measured internal resistance  $R_i$  values versus  $R_i$  values obtained from the optimization script at 10% step SOC for discharge pulses.



At very low SOC, the cell behaves differently and the voltage decreases exponentially when there is a discharge current. A detailed study at very low SOC is required. Either the structure of the SOEC model has to be changed at very low SOC or the method of obtaining the parameters needs to be further verified. This is scope of future work. Also in the context of the work the discharge VOC was used in the discharging direction of the HPPC profile and the charge VOC was used in the charging direction.

This could be done as there was apriori knowledge of the charging direction and voltage simulation was done off-line. However for on-line real-time simulation of the voltage response when the current measurements are captured as in a BMS application, this is not possible. In most cases, other researchers have resorted to using the average VOC method. But it has been observed that the use of average VOC can produce suboptimal results due to the hysteresis effect. A more sophisticated method such as the use of enhanced self-correcting cell model method where there is a hysteresis rate constant as stated in [22] is needed and this is also the scope of future work

### 3.6 Investigation on cell chemistry

The cell characterization is strongly dependent on its chemistry. The criterion for choice of cell chemistry depends on the EV application, specific energy and specific power, safety, cost and its lifespan. Some chemistry have high specific energy, low specific and viz., different discharge characteristics, different charging protocol and their performance is influenced by state of charge (SOC) and temperature. A universal battery model with same set of parameters is not possible to describe the dynamic behaviour of different cell chemistries.

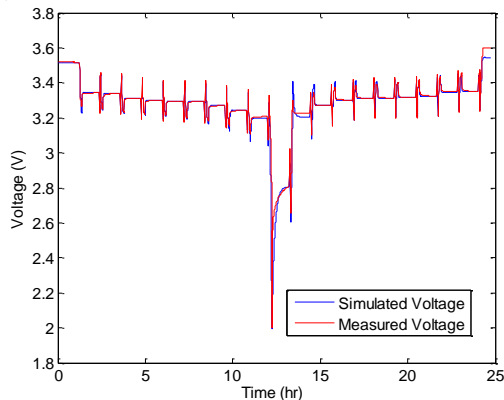


Figure 10: Measured and simulated voltage response of the SOEC model for Cell Type 1.

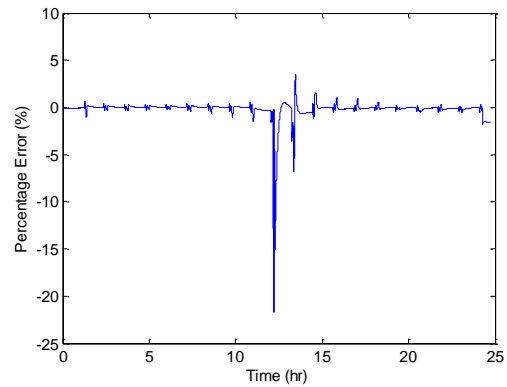


Figure 11: SOEC Modelling Error.

This section describes the dynamic behaviour of different cell chemistry Lithium-ion cells at various SOC as stated in Tab.2. A study was made on VOC behaviour of these chemistries. The VOC data is obtained from HPPC tests at every 10% SOC step when the cells are discharged, followed by a 1 hour complete pause to attain voltage and temperature equilibrium. Fig.12 shows the comparison of VOC plotted vs. SOC at 10% SOC interval step.

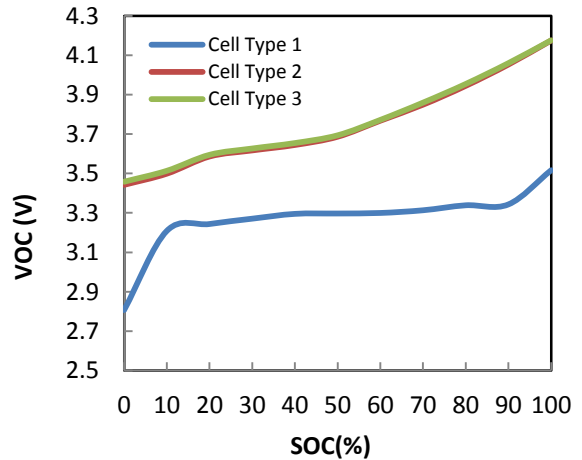


Figure 12: VOC vs. SOC for different cell chemistry.

LCO and LMO chemistries exhibit sloping characteristics of SOC vs. open circuit voltage. However the open circuit voltage behaviour of LFP shows complete contrast to other two chemistries. The open circuit voltage increases between SOC 0 and 20%. Then it goes into a plateau region between 20 and 90% SOC, again it increases above 90% SOC. LFP exhibits two phase transition during charging and discharging. During this process, the electrode potential shows a minor change in VOC with respect to SOC change due to constant lithium concentration within the phase regions [23, 24]. However in LCO and LMO

chemistries, lithium insertion and de-insertion take place without two phase transition.

A SOEC model is developed for LCO and LMO chemistries by repeating the HPPC test. Three sample cells were tested from each of the chemistry for statistical reliability of the measured data. The circuit parameters are fitted in Matlab as described in [section 3.4](#). The results of the fitting parameters are then plotted for the chemistries described in [Tab.2](#). [Fig.13\(a\)-\(e\)](#) show the plot of circuit parameters against SOC. The internal resistance  $R_i$  is very low ( $\sim 20$  m $\Omega$ ) for cell type 1 when compared to cell type 2 and cell type 3. This is a typical characteristic of high power Lithium-ion cells. The resistance  $R_i$  for the three chemistries shows similar behaviour throughout the SOC window. It is almost flat from 100% - 20 % SOC and increases below 20% SOC, maximum at completely discharged state [\[25\]](#). The resistance  $R_1$  which contributes to charge transfer reaction has the least value compared to other resistance  $R_i$  and  $R_2$ . It also shows a similar trend as  $R_i$ . The resistance  $R_2$  increases abruptly when the cells are discharged beyond 20%. SOC. The diffusion process becomes a limitation factor when the cell is near complete discharge. The values of Capacitance  $C_1$  and  $C_2$  generally increase with increase in SOC, but at some SOC it does not change significantly or its value decreases.

The model is validated by simulating the voltage behaviour for different C-Rate and comparing them with the measurement values. [Fig.13\(f\)](#) shows the plot of measured and simulated voltage against the discharge capacity for LCO chemistry. The simulated voltage shows good agreement with the measured values. However there is a deviation in the simulated value below 20% SOC. This deviation can be correlated to the fitting parameter values below 20% SOC. From these results, it can be understood that the circuit parameter values are the intrinsic property of the cell chemistry. A more detailed understanding of chemistry is required to quantify the values of circuit parameters. Therefore, a SOEC model is applicable for all practical purposes to study the dynamic behaviour of the cells having different chemistry.

## 4 Conclusions

An extensive testing method for the development and validation of a SOEC model has been presented. A method to identify the parameters for the SOEC model from characteristic HPPC power test measurements is also described. The performance of the SOEC model is good producing very low modelling errors as low as less than 3% in the SOC range from 20-80%. This is sufficient to capture the dynamics of most lithium-ion cells for most BMS applications as most EVs and HEVs typically operate in that range.

The current pulse step technique was also described. This method is useful for verifying  $R_i$  obtained from the parameter characterization method. It is also verified that the SOEC model is valid for cells from different chemistries but the model parameters have to be determined individually for each of the cell chemistry as this is an intrinsic property of the cell.

## Acknowledgments

This work has been done in the framework of CREATE research programme funded by the Singapore National Research Foundation (NRF).

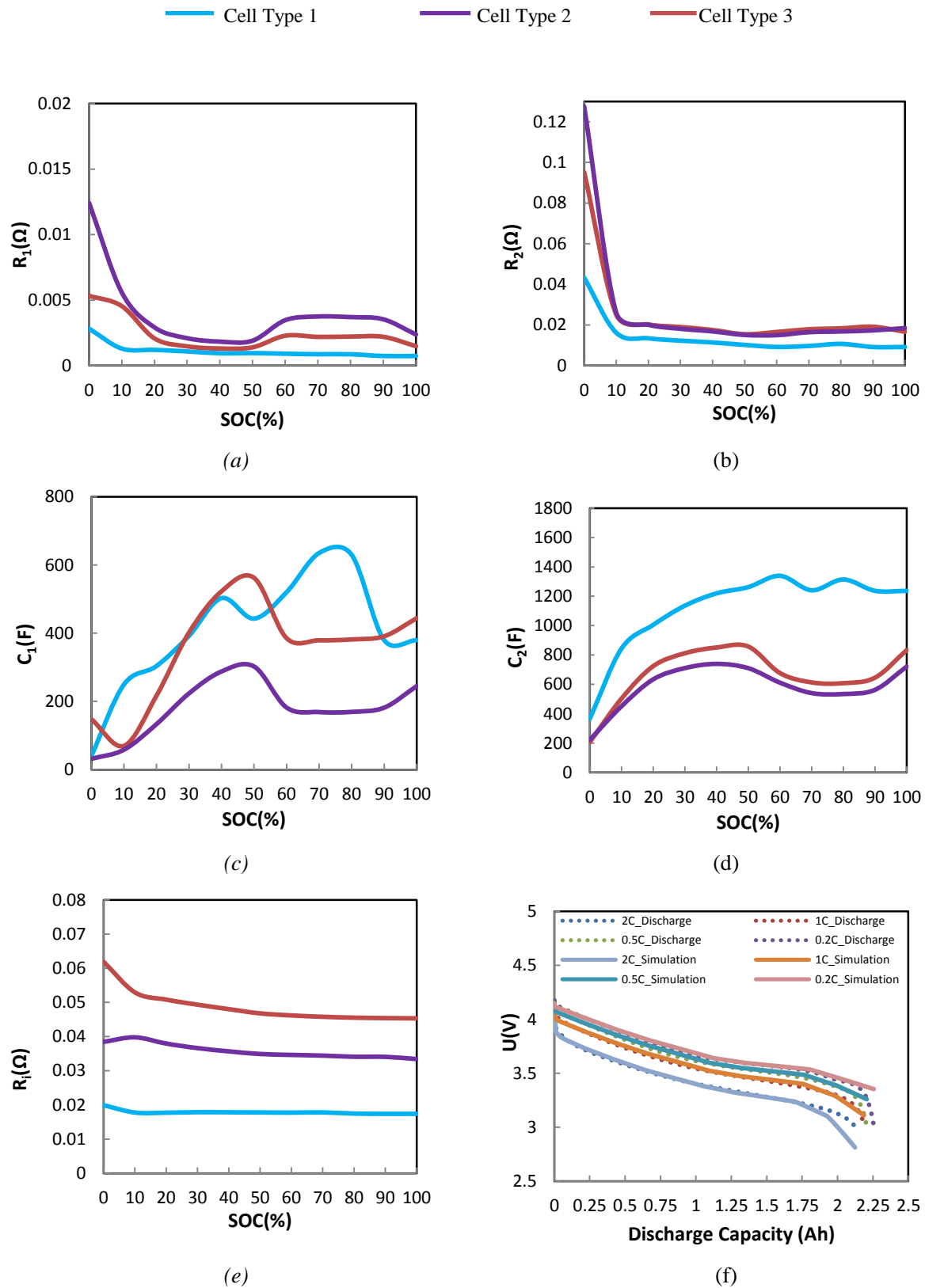


Figure 13: Comparison of (a) Short Transient Resistance ( $R_1$ ), (b) Long Transient Resistance ( $R_2$ ), (c) Short Transient Capacitance ( $C_1$ ), Long Transient Capacitance ( $C_2$ ) and (d) Internal Resistance ( $R_i$ ) for the given chemistries as function of SOC. (f) shows the plot of Measurement and Simulated Voltage vs. Discharge Capacity of Cell Type 2 at different C-Rates.

## References

- [1] J. Newman and W. Tiedemann, *Porous-Electrode Theory with Battery Applications*, AIChE Journal, 1975. **21**(1): p. 25-41.
- [2] M. Doyle, T. Fuller, and J. Newman, *Modeling of galvanostatic charge and discharge of the lithium/ polymer/insertion cell*, Journal of the Electrochemical Society, 1993. **140**(6): p. 1526-1533.
- [3] Xiao Hu, et al., *A Foster network thermal model for HEV/EV battery modeling*, IEEE Transactions on Industry Applications, 2011. **47**(4): p. 1692-1699.
- [4] Cai Long and R.E. White, *Mathematical modeling of a lithium ion battery with thermal effects in COMSOL Inc. Multiphysics (MP) software*, Journal of Power Sources, 2011. **196**(14): p. 5985-5989.
- [5] C.M. Shepherd, *Design of Primary and Secondary cells*, Journal of the Electrochemical Society, 1965. **112**: p. 657-664.
- [6] O. Tremblay, L.A. Dessaint, and A.I. Dekkiche. *A Generic Battery Model for the Dynamic Simulation of Hybrid Electric Vehicles*, in *IEEE Vehicle Power and Propulsion Conference*. 2007.
- [7] Mathworks Inc. *MATLAB SimPowerSystems User's Guide, Version 5.4 (R2011a)*. Available from: <http://www.mathworks.com/access/helpdesk/help/toolbox/phymod/powersys/>.
- [8] V.H. Johnson, *Battery performance models in ADVISOR*, Journal of Power Sources, 2002. **110**(2): p. 321-329.
- [9] S. Jiang, *A Parameter Identification Method for a Battery Equivalent Circuit Model*, SAE Technical Paper, 2011. **2011-01-1367**.
- [10] Chen Min and G.A. Rincon-Mora, *Accurate electrical battery model capable of predicting runtime and I-V performance*, IEEE Transactions on Energy Conversion, 2006. **21**(2): p. 504-511.
- [11] L. Jaemooon, et al. *Modeling and Real Time Estimation of Lumped Equivalent Circuit Model of a Lithium Ion Battery*, in *Power Electronics and Motion Control Conference, 2006. EPE-PEMC 2006. 12th International*. 2006.
- [12] S. Lee, et al., *State-of-charge and capacity estimation of lithium-ion battery using a new open-circuit voltage versus state-of-charge*, Journal of Power Sources, 2008. **185**(2): p. 1367-1373.
- [13] Mathworks Inc. *Matlab Simscape 3.5 (R2011a)*. Available from: <http://www.mathworks.com/products/simscape/>.
- [14] EUCAR Traction Battery Working Group, *Specification of Test Procedures for Hybrid Electric Vehicle Traction Batteries*, September 1998.
- [15] EUCAR Traction Battery Working Group, *Specification of Test Procedures for High Voltage Hybrid Electric Vehicle Traction Batteries*, January 2005.
- [16] G.L. Plett. *Results of Temperature-Dependent LiPB Cell Modeling*, in *Proceedings of 21st Electric Vehicle Symposium (EVS21)*. April 2005. Monaco.
- [17] Idaho National Engineering & Environmental laboratory, *FreedomCAR Battery Test Manual for Power-Assist Hybrid Electric Vehicles*, Oct 2003.
- [18] S. Yang, et al., *Performance of LiFePO4 as lithium battery cathode and comparison with manganese and vanadium oxides*, Journal of Power Sources, 2003. **119-121**(0): p. 239-246.
- [19] P. Keil, *Development of a battery model for the analysis of energy management strategies for electric vehicles*, in *Institute for Electrical Energy Storage Technology 2010*, Technische Universität München.
- [20] K. Wolter, *Auslegung einer Pufferbatterie für das 12-V-Bordnetz eines Elektrofahrzeugs*, in *Institute for Electrical Energy Storage Technology 2011*, Technische Universität München.
- [21] H.-G. Schweiger, et al., *Comparison of several methods for determining the internal resistance of lithium ion cells*, Journal of Sensors, 2010. **10**(6): p. 5604-5625.
- [22] R.A. Jackey, G.L. Plett, and M.J. Klein, *Parameterization of a Battery Simulation Model Using Numerical Optimization Methods*, 2009, SAE International.
- [23] V. Srinivasan and J. Newman, *Discharge model for the lithium iron-phosphate electrode*, The Journal of Electrochemical Society, 2004. **151**(A1517).
- [24] M.A. Roscher, J. Vetter, and D.U. Sauer, *Cathode material influence on the power capability and utilizable capacity of next generation lithium-ion batteries*, Journal of Power Sources, 2010. **195**(12): p. 3922-3927.
- [25] B. Yann Liaw, et al., *Modeling of lithium ion cells—A simple equivalent-circuit model approach*, Journal of Solid State Ionics, 2004. **175**(1-4): p. 835-839.

## Authors



Suguna Thanagasundram earned her B.Eng. in electrical and electronic engineering from National University of Singapore. She completed her MSc and PhD degrees from the University of Leicester UK in 2003 and 2007 respectively. She is currently a Research Fellow in TUM CREATE in Singapore, working in the area of electrical storage systems.



Tanja Teutsch received her B.Sc. in Electrical Engineering and Information Technology from Technische Universität München (TUM) in 2012. She is currently pursuing a Dipl.-Ing. degree at TUM and writing her thesis on battery modelling and battery state estimation in TUM CREATE in Singapore.



Raghavendra Arunachala earned his B.Eng. in electrical and electronic engineering from Visveswaraya Technological University, India. He completed his M.Sc from Rheinische Westfälische Technische Hochschule (RWTH) Aachen University, Germany in 2011. He is currently a doctoral student in TUM CREATE, Singapore, working in the area of electrical energy storage systems



Andreas Jossen earned his doctorate, dealing with "Management of photo-voltaic plants using energy storage systems" at University of Stuttgart. From 1994 he was group leader for different battery related topics with ZSW, Ulm. Since 2010 he is full professor at the Institute for Electrical Energy Storage Technology, TUM.



Kamyar Makinejad received his B.Sc. in electrical engineering in 2007 from Shiraz University, Iran. He earned his MSc degree from Leibniz University of Hanover, Germany in 2011 respectively. He is currently a Research Associate in TUM CREATE in Singapore and pursuing his PhD with the Technical university of Munich. His research interest is battery diagnostic and state determination in EV applications.